Magnetic Field Measurements and Reconstruction of Very Broadband Electron Spectrometer for Plasma Experiments

J. W. Phillips, B. Naranjo, O. Williams, J. A. Phillips, G. Andonian, A. Fukasawa, Y. Kang, P. Manwani, J. Rosenzweig

UCLA Dept. of Physics & Astronomy

Advanced Accelerator Conference 2026
Los Angeles, 2026 July 28

Motivation

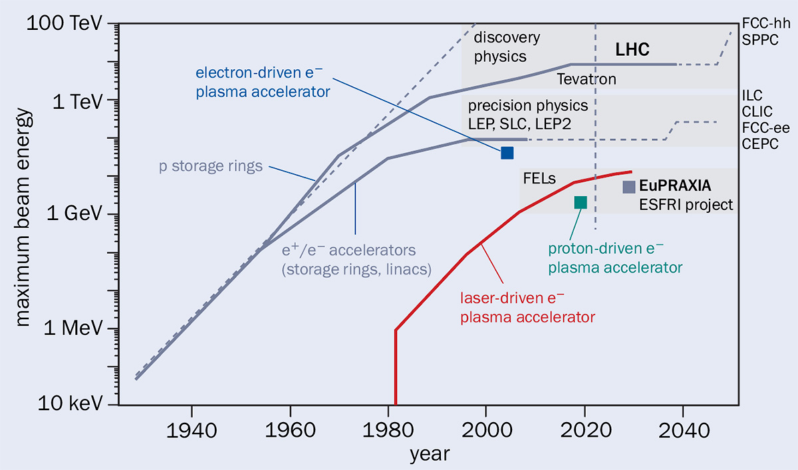

Assmann et al., CERN Courier (2023)

- Traditional RF acceleration techniques have leveled off.
- Strong need for more compact acceleration.

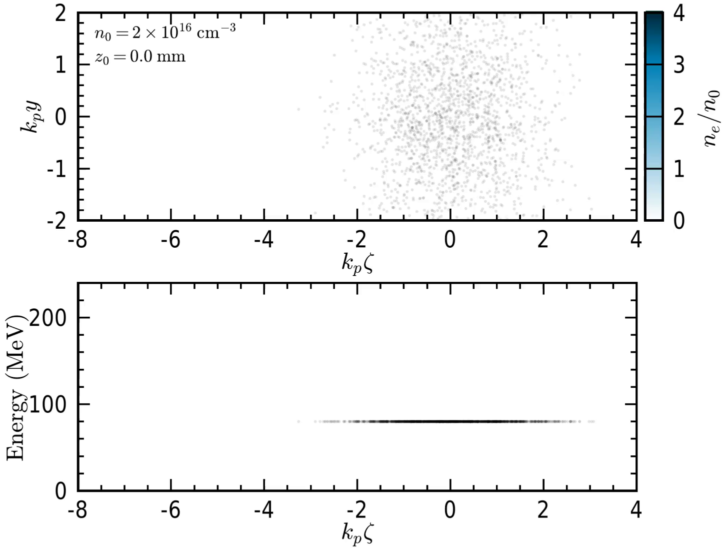

- Black particles are the incoming electrons.
- Blue background is plasma density.

Plasma Wakefield Acceleration

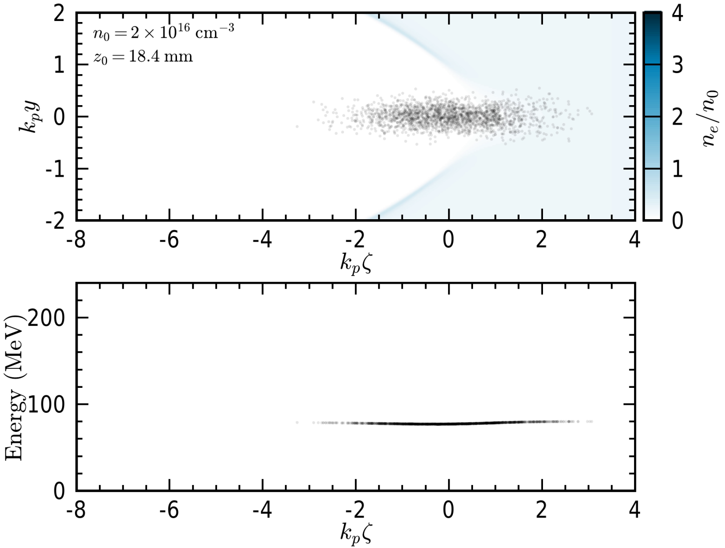

- Black particles are the incoming electrons.
- Blue background is plasma density.

Plasma Wakefield Acceleration

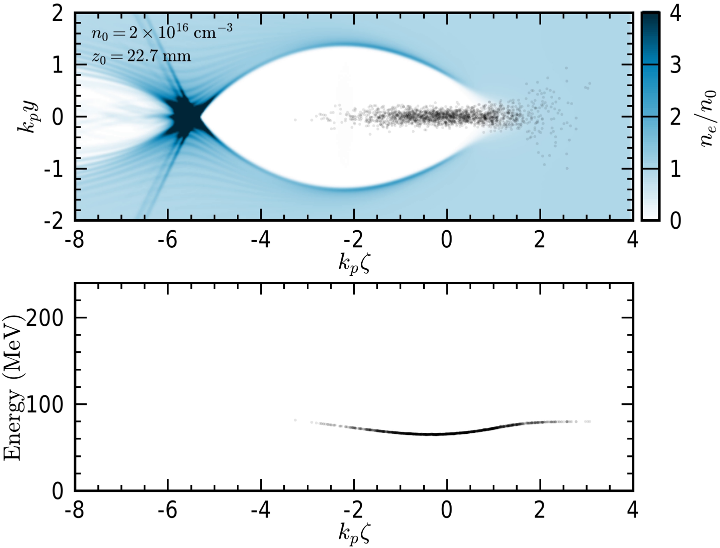

- Black particles are the incoming electrons.
- Blue background is plasma density.

Plasma Wakefield Acceleration

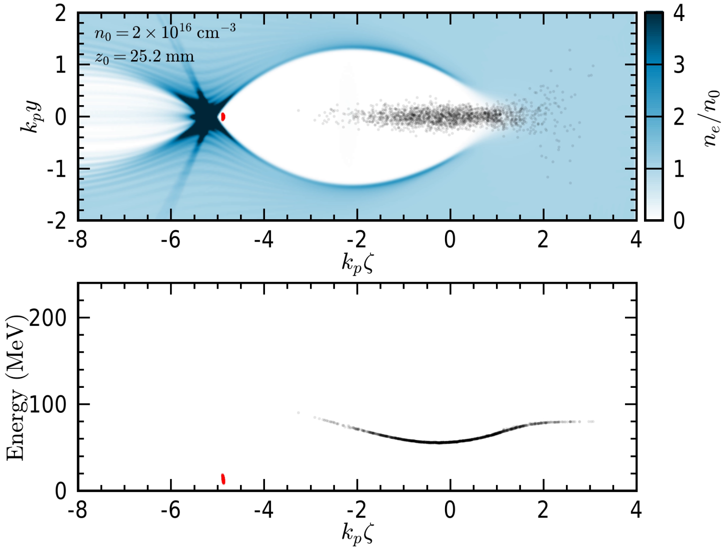

- Black particles are the incoming electrons.
- Blue background is plasma density.

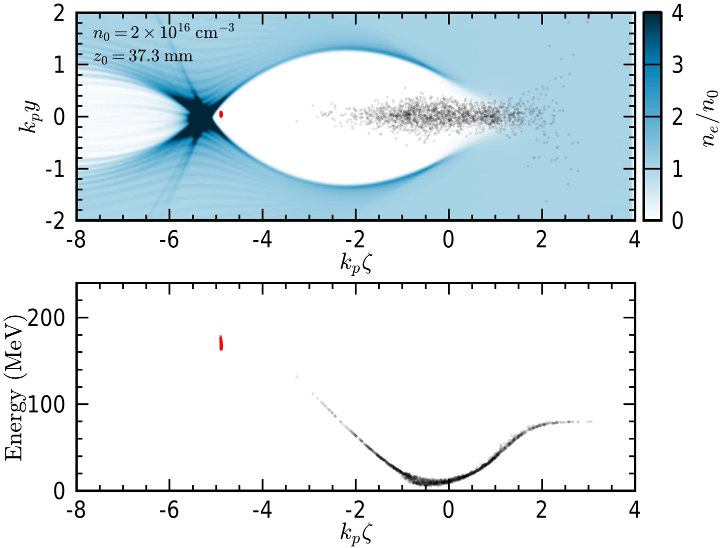

- Black particles are the incoming electrons.
- Blue background is plasma density.

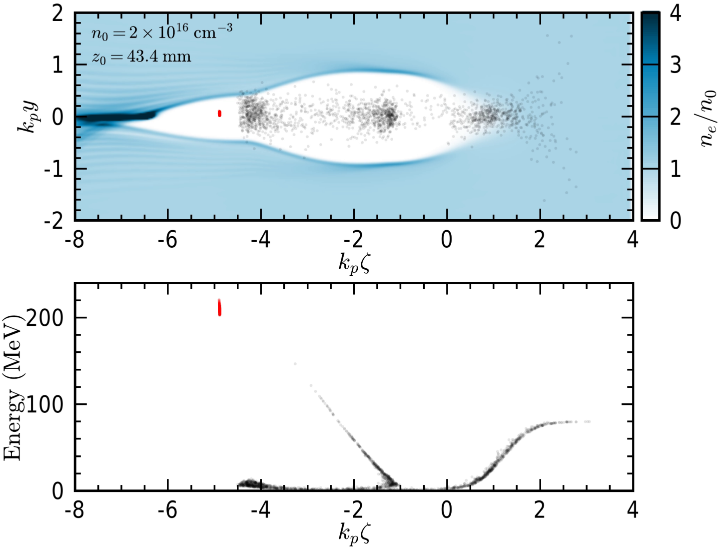

- Black particles are the incoming electrons.
- Blue background is plasma density.

Broadband Spectrometer

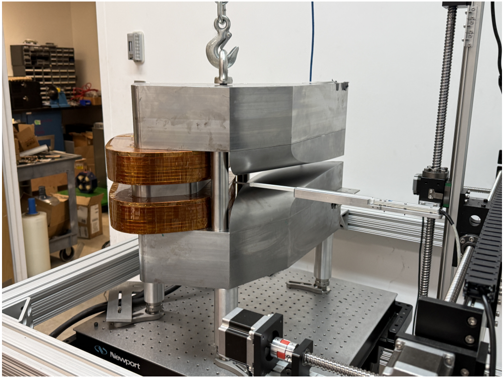

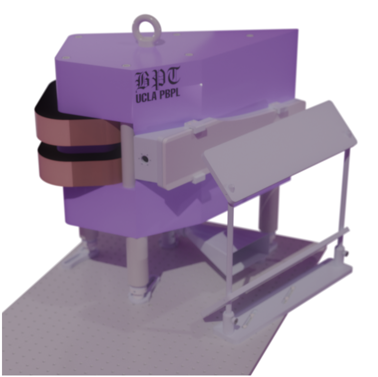

- Need a very broadband spectrometer to fully characterize PWFA's energy in a single-shot
- Traditional dipole spectrometers will not be sufficient
- The beta spectrometer (BPT) fulfills the strict energy requirements
- Left image shows the assembled version being measured by a Hall probe, the right image shows the 3D model

Sextupole Fields

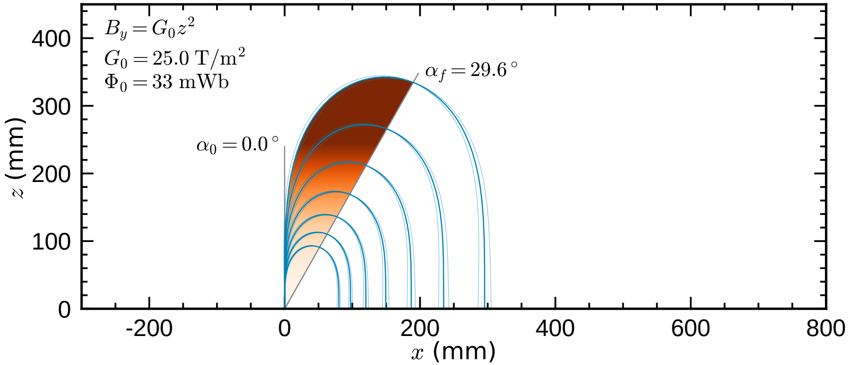

- In sextupole fields, there exists mechanically similar solutions such that the length scales with the cube root of momentum
- This allows for much broader compression compared to dipole fields where length scales linearly with momentum

Sextupole Fields

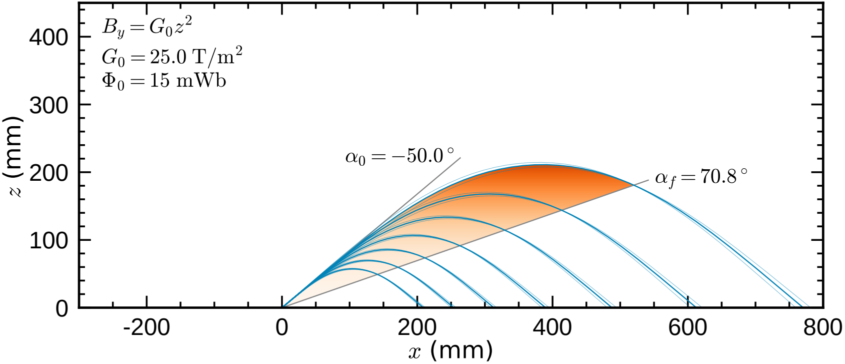

- As fields quadratically grow further into the sextupole, sending the electron beam in the fields at an angle can help minimize the magnetic flux used.
- How do these fields correspond to the actual magnet?

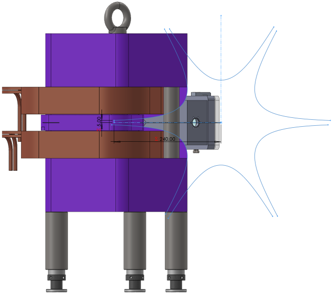

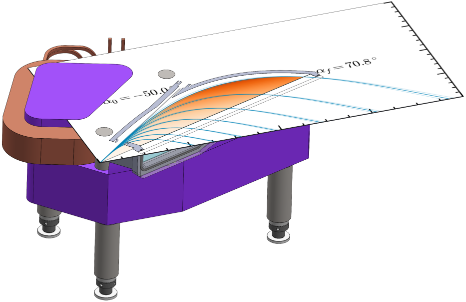

- BPT's pole tips are curved to optimally generate sextupole fields.
- The electron beam comes in at a 50.0° angle with respect to BPT's pole tips.
- BPT has a modular design to allow future upgrades/replacements to the pole tips and core.
- Learn more about BPT's sextupole design during Dr. Brian Naranjo's talk at 5:20pm!

Hysteresis

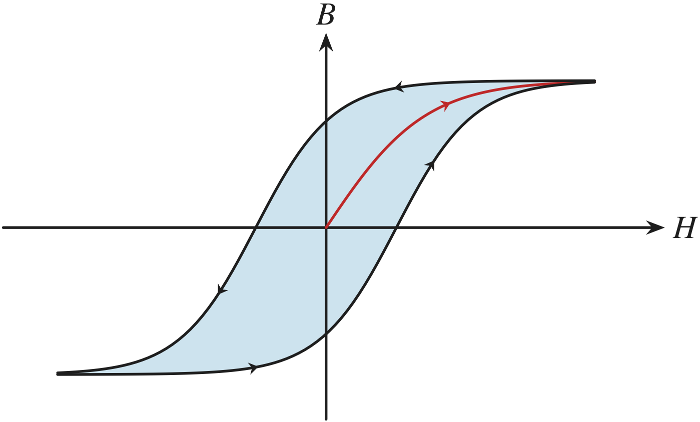

- Past states of magnets affect current ones.
- Need for normalization procedure!

Hysteresis

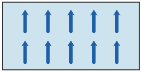

1 Saturation $(+B_s)$
all domains aligned

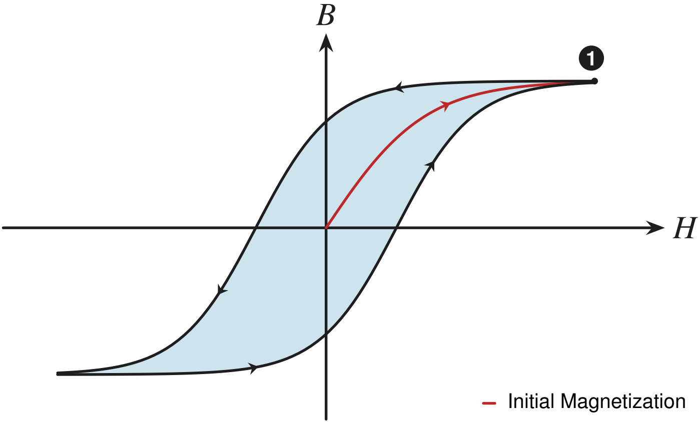

- Past states of magnets affect current ones.
- Need for normalization procedure!

Hysteresis

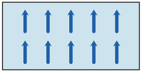

1 Saturation $(+B_s)$
all domains aligned

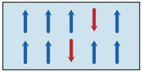

2 Remanence $(+B_r)$
$H=0$, most stay aligned

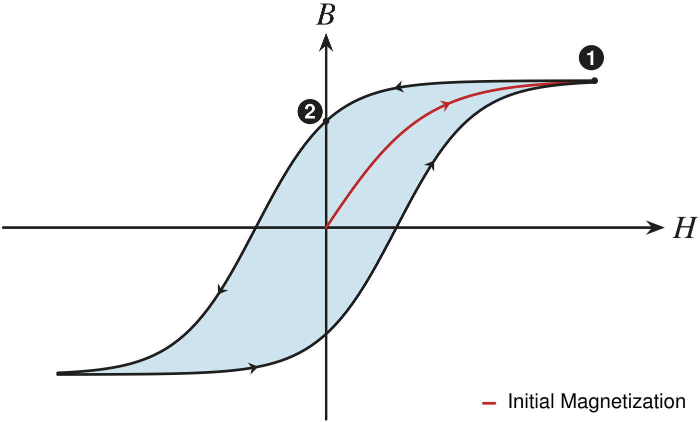

- Past states of magnets affect current ones.
- Need for normalization procedure!

Hysteresis

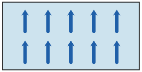

1 Saturation $(+B_s)$
all domains aligned

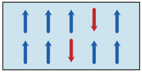

2 Remanence $(+B_r)$
$H = 0$, most stay aligned

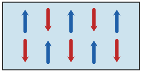

3 Coercivity $(-H_c)$
equal split, $B = 0$

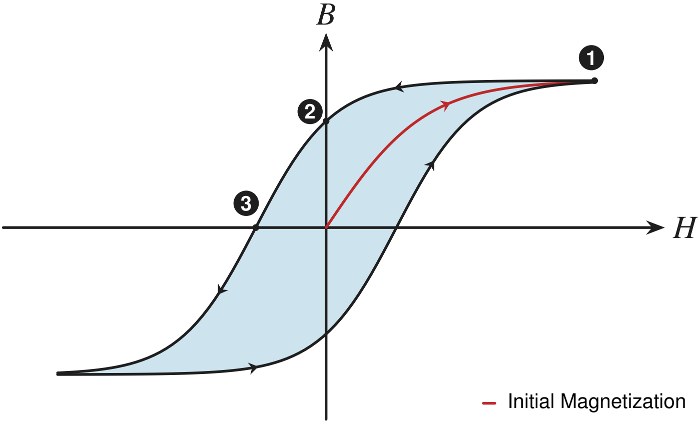

- Past states of magnets affect current ones.
- Need for normalization procedure!

Hysteresis

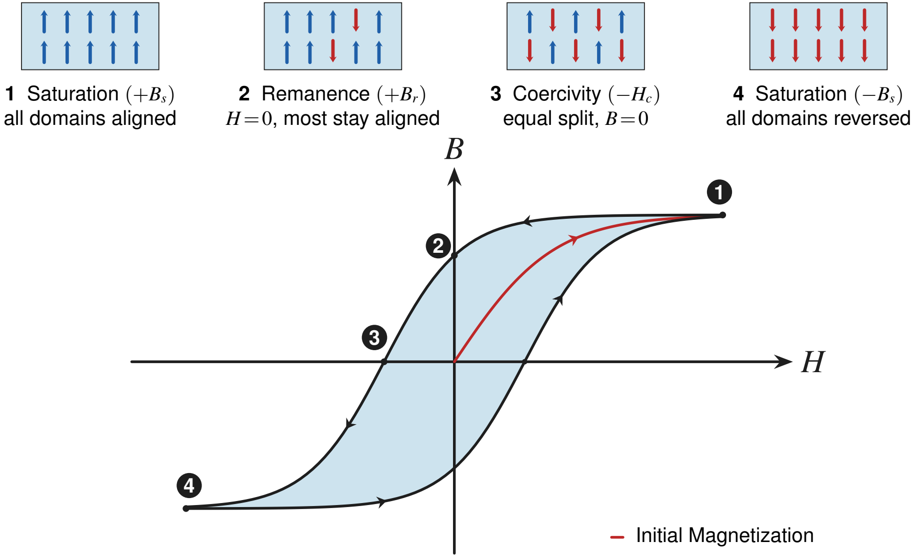

- Past states of magnets affect current ones.
- Need for normalization procedure!

Need for normalization

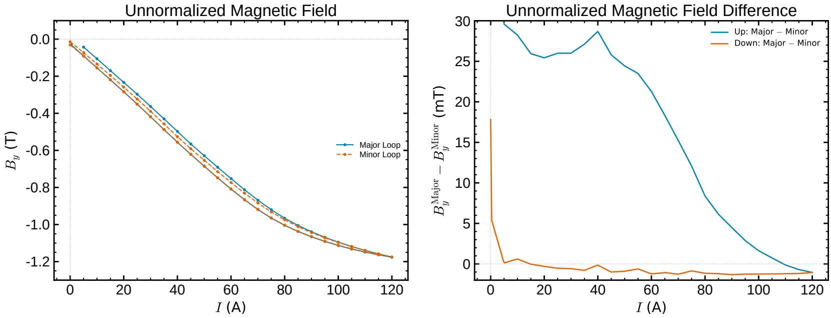

- Above plots illustrate the effect of this hysteresis.
- The major loop is measurements from when the magnet is on the 120 A bipolar ramp hysteresis curve and the minor loop is when it is on the 120 A unipolar ramp curve.
- Because of this hysteresis, it is critical for the magnet to be properly normalized before any precise measurements.

Normalization of the Magnet

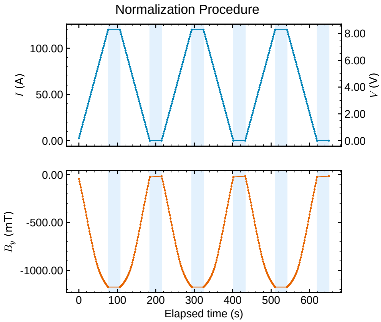

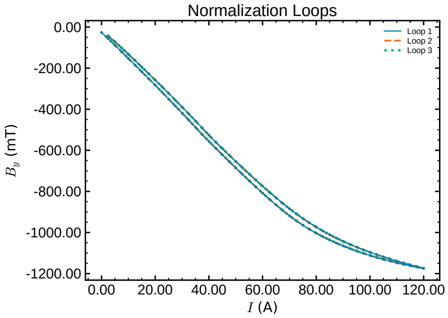

- Opted for a ~ 1.5 A/s current ramp up and down from 0 A to 120 A three times.
- Current is held at 120 A and 0 A for 30 s.
- Right figure illustrates this normalization on the peak field point.

Normalization of the Magnet

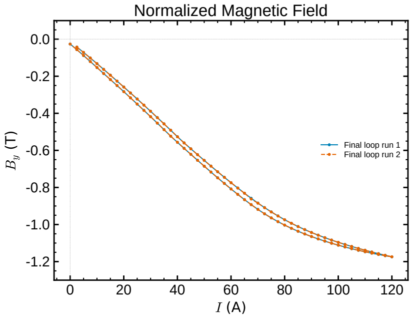

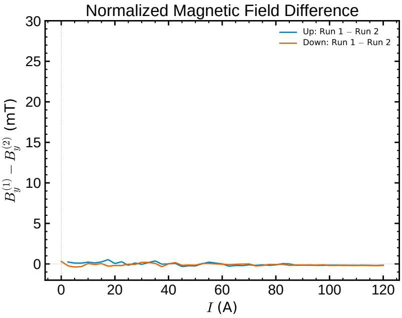

- The normalization procedure results in great reproducibility of the magnet.
- Large improvement compared to unnormalized magnet.

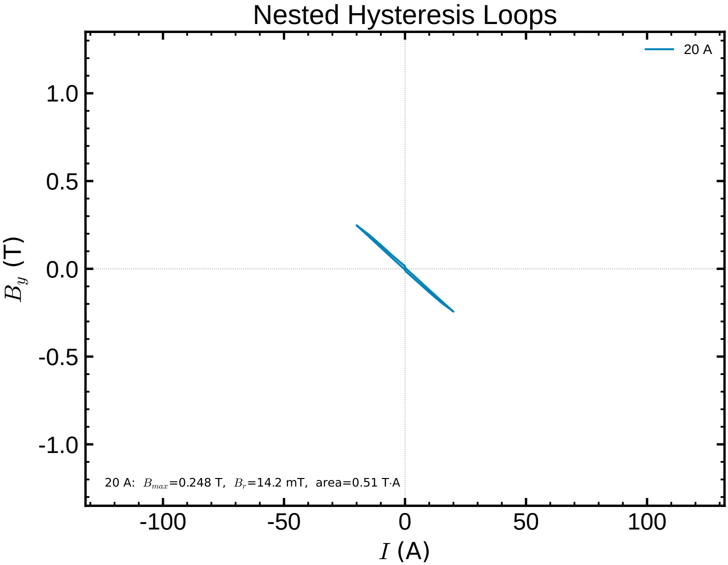

- 20 A loop: $B_{max} = 0.248$ T, $B_r = 14.2$ mT, area $= 0.51$ T·A

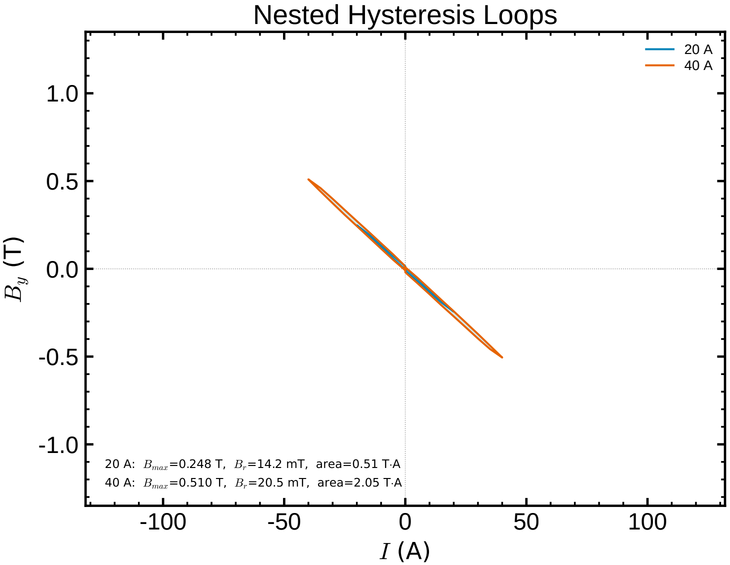

- 40 A loop: $B_{max} = 0.510$ T, $B_r = 20.5$ mT, area $= 2.05$ T·A

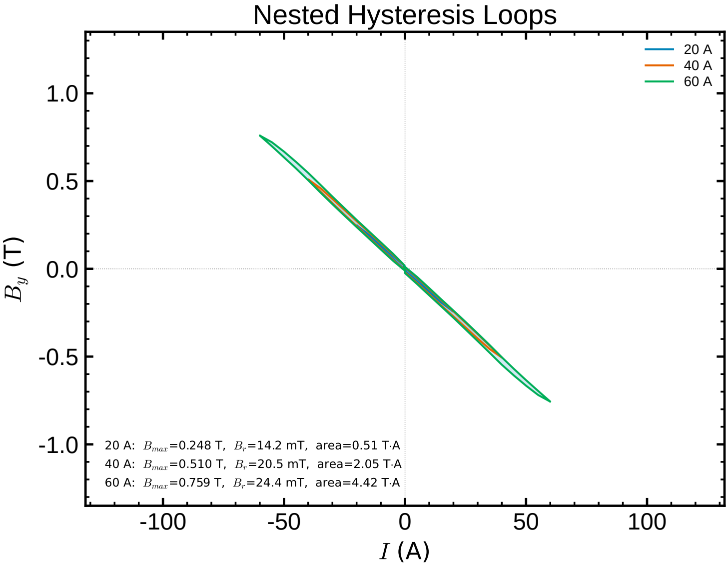

- 60 A loop: $B_{max} = 0.759$ T, $B_r = 24.4$ mT, area $= 4.42$ T·A

Hysteresis

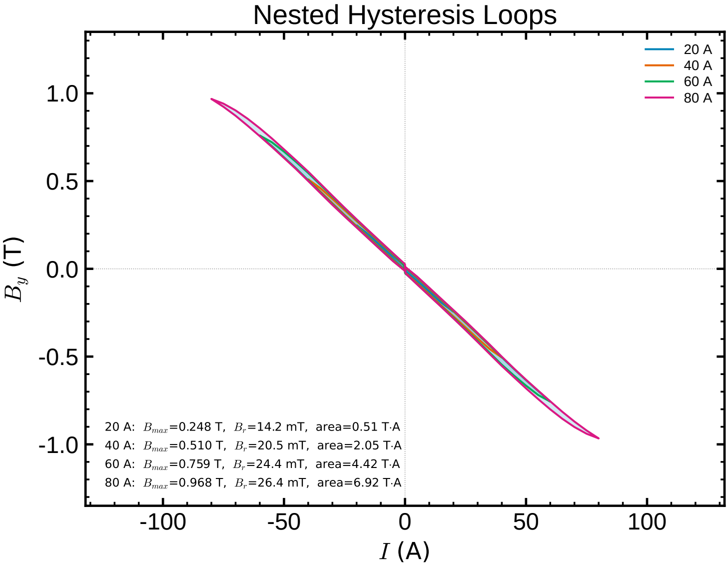

- 80 A loop: $B_{max} = 0.968$ T, $B_r = 26.4$ mT, area $= 6.92$ T·A

Hysteresis

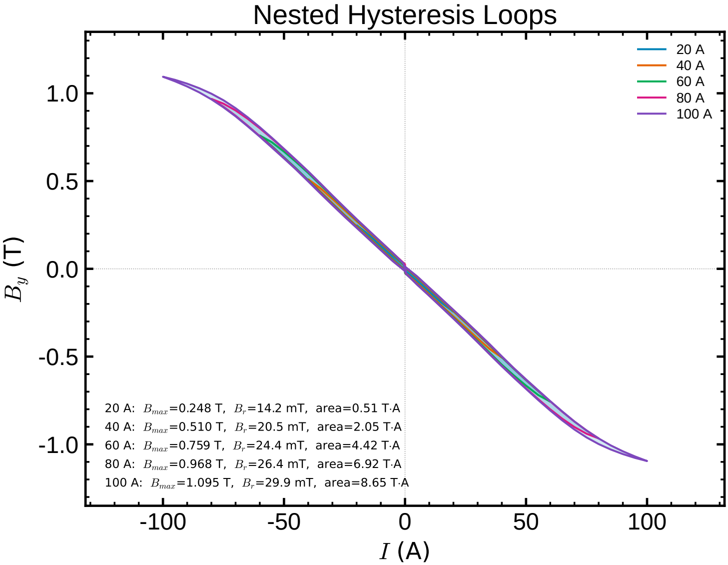

- 100 A loop: $B_{max} = 1.095$ T, $B_r = 29.9$ mT, area $= 8.65$ T·A

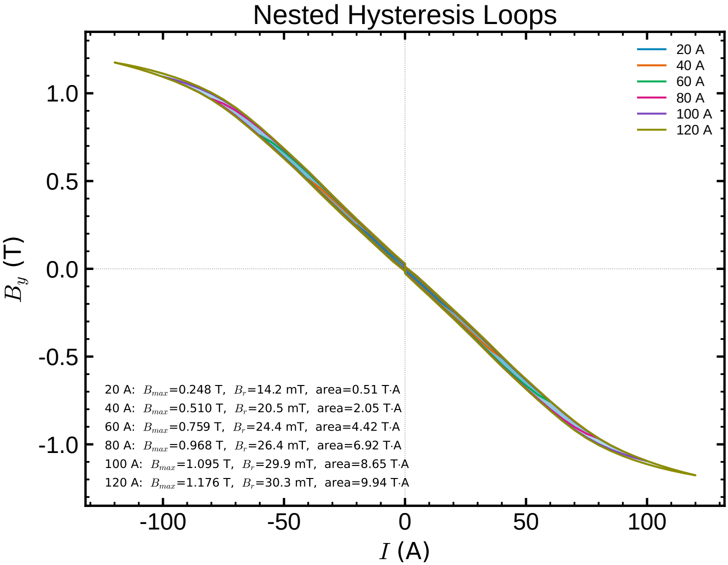

- 120 A loop: $B_{max} = 1.176$ T, $B_r = 30.3$ mT, area $= 9.94$ T·A

Field Maps

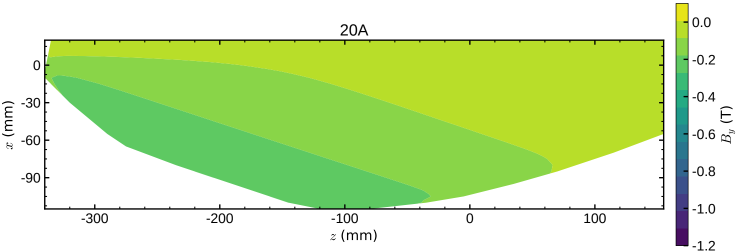

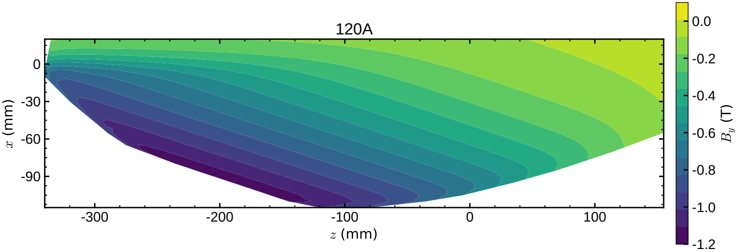

- 2D magnetic field scans were taken from 0 A to 120 A in 20 A increments.
- The lowest and highest currents are shown above
- These can be used to evaluate the saturation

Field Maps

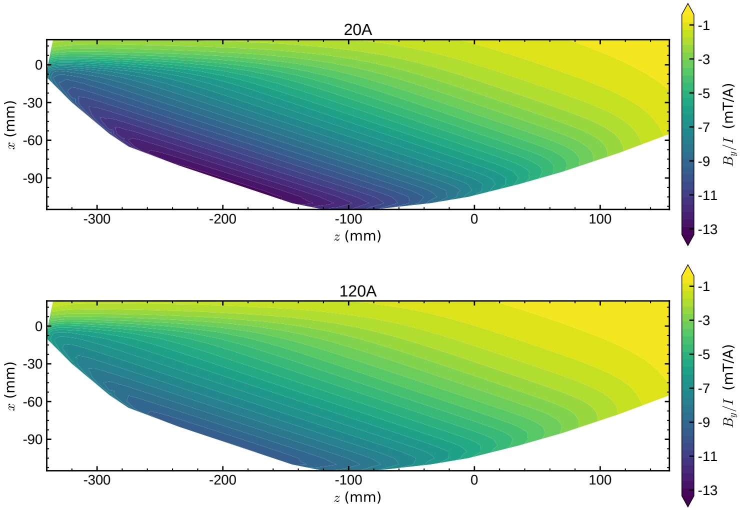

- Normalizing the fields by the currents
- If there was no saturation, then these plots would be equivalent
- The large amount saturation in the high-field regions is due to the pole tips, whereas the lesser amount of saturation in the low-field regions is due to the core.

Field Maps

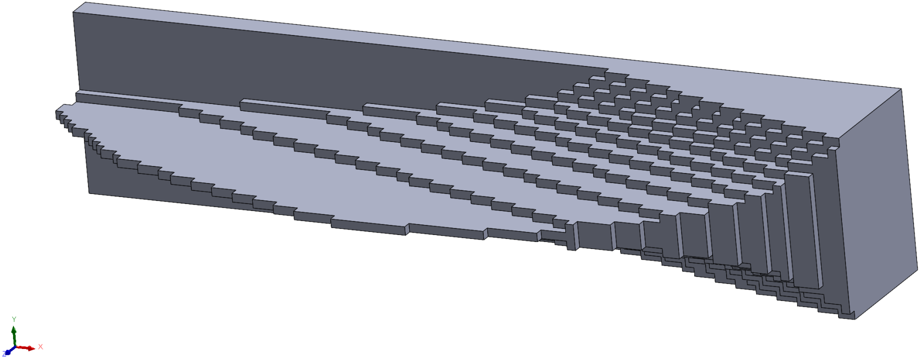

- Took 3D magnetic field maps at 0 A, 80 A, 100 A, 120 A.
- 10 mm grid due to time restraints, took around 5 hours.
- Would take much longer on 1 mm grid.
- Need for reconstruction.

Maxwell's Equations in a Current-Free Region

In a current-free region, Maxwell's equations reduce to:

$$\nabla \times \mathbf{B} = 0 \implies \mathbf{B} = -\nabla\Phi \tag{1}$$

$$\nabla \cdot \mathbf{B} = 0 \implies \nabla^2\Phi = 0 \tag{2}$$

- Φ is the magnetic scalar potential and $\mathbf{B}$ is the magnetic field
- The fact that there is no current in the spot we are measuring allows us to represent the magnetic field with a scalar potential
- The lack of magnetic monopoles implies that this scalar potential satisfies Laplace's equation
- We can have our reconstruction Maxwell-consistent by utilizing harmonic functions.
- Using a harmonic polynomial basis.

Magnetic Field Reconstruction

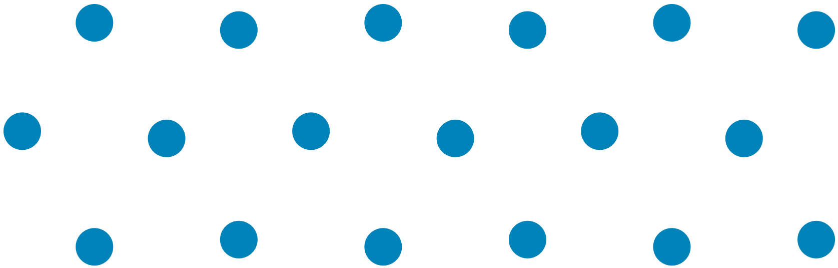

Measured Field Points

Blue dots: known field values on scattered, non-uniform grid. We need to accurately predict the magnetic field at any unmeasured point.

Magnetic Field Reconstruction

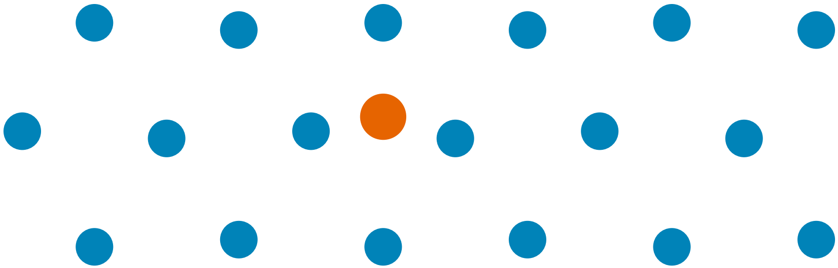

Query Point $\mathbf{x}_q$

Orange dot: location where we want the field but have no measurement. A global fit can oversmooth the data, resulting in less accuracy in fringe regions.

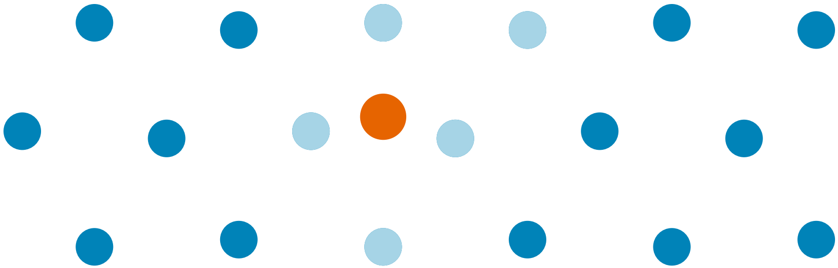

1. *k*-Nearest Neighbors Search

For each query point $\mathbf{x}_q$, find $k = 15$ nearest neighbors $\mathcal{N}_q$ via *k*-nearest neighbor (KNN) search on axis-normalized positions.

Magnetic Field Reconstruction

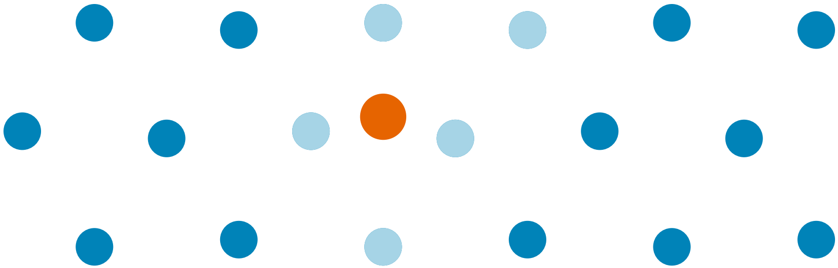

2. Build Basis Matrix

Construct $\mathbf{A}_q \in \mathbb{R}^{3k \times N}$ $(N = 45)$ from harmonic polynomials H_n:

$$\mathbf{A}_q = \begin{pmatrix} \partial_x H_1(\tilde{\mathbf{x}}_1) & \cdots & \partial_x H_N(\tilde{\mathbf{x}}_1) \\ \partial_y H_1(\tilde{\mathbf{x}}_1) & \cdots & \partial_y H_N(\tilde{\mathbf{x}}_1) \\ \partial_z H_1(\tilde{\mathbf{x}}_1) & \cdots & \partial_z H_N(\tilde{\mathbf{x}}_1) \\ \vdots & & \vdots \\ \partial_z H_1(\tilde{\mathbf{x}}_k) & \cdots & \partial_z H_N(\tilde{\mathbf{x}}_k) \end{pmatrix}$$

where $\tilde{\mathbf{x}}_i = \mathbf{x}_i / r_0$, $r_0 = \max_{\mathcal{N}_q} \|\mathbf{x}_i\|$.

Magnetic Field Reconstruction

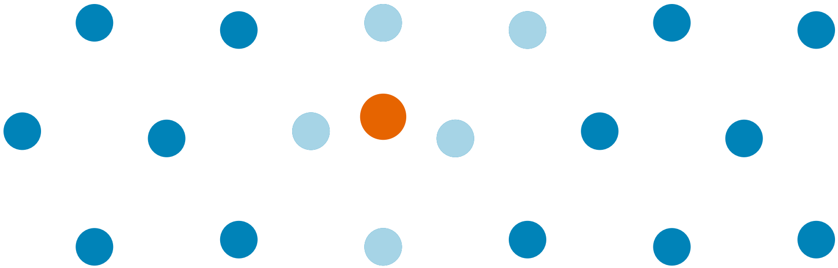

3. Tikhonov Regularization

Solve ($\lambda = 10^{-11}$):

$$\mathbf{c}_q = \left(\mathbf{A}_q^\top \mathbf{A}_q + \lambda \mathbf{I}\right)^{-1} \mathbf{A}_q^\top \mathbf{b}_q$$

where $\mathbf{b}_q$ are the measured field values at $\mathcal{N}_q$.

Magnetic Field Reconstruction

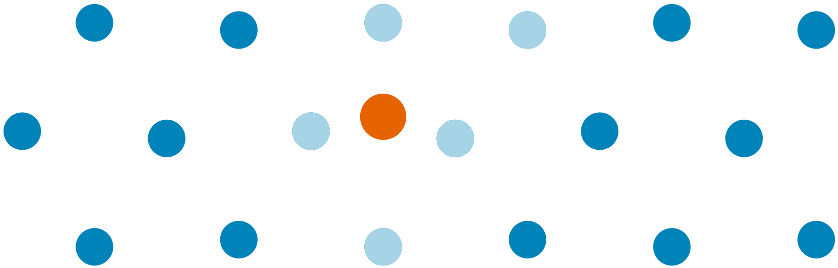

4. Predict

Predict the magnetic field at the query point $\mathbf{B}(\mathbf{x}_q)$,

$$\mathbf{B}(\mathbf{x}_q) = \mathbf{A}'_q \, \mathbf{c}_q, \quad \mathbf{A}'_q \in \mathbb{R}^{3\times N},$$

where $\mathbf{A}'_q$ is the matrix from step 2 in a new neighborhood $\mathcal{N}'_q$ that only contains the query point.

Reconstruction Accuracy

The L1 norm of the reconstruction error is defined as:

$$L_1 = \sum_{i=1}^{N} \left[|B_x^{\text{pred}} - B_x^{\text{true}}| + |B_y^{\text{pred}} - B_y^{\text{true}}| + |B_z^{\text{pred}} - B_z^{\text{true}}| \right]_i \tag{3}$$

Method	**L1 (T)**	**RMS (mT)**	**Mean (mT)**	**Median (mT)**	**Max (mT)**
Local harmonic	**1.923**	**4.41**	**0.511**	**0.028**	145.7
Linear	6.360	6.22	1.718	0.165	81.8
RBF linear	7.058	5.31	1.876	0.256	105.2
RBF cubic	3.203	4.53	0.852	0.099	139.6
RBF thin plate spline	3.907	4.51	1.039	0.115	133.3
RBF quintic	2.816	4.70	0.749	0.100	148.8

- Compared results to linear interpolation and radial basis function (RBF) interpolation with different kernels
- Local harmonic wins on L1, RMS, Mean, and Median. Around $3.3\times$ better L1 than linear interpolation
- Median 28 μT = 0.002% of peak field
- Performs better on more difficult points

Percentile Errors

Per-point error of ith point: $\epsilon_i = \sqrt{(B_x^{\text{pred}} - B_x^{\text{true}})^2 + (B_y^{\text{pred}} - B_y^{\text{true}})^2 + (B_z^{\text{pred}} - B_z^{\text{true}})^2}$

Method	**p50 (mT)**	**p75 (mT)**	**p90 (mT)**	**p95 (mT)**	**p99 (mT)**
Local harmonic	**0.111**	**0.346**	**1.633**	**4.778**	30.073
Linear	0.615	3.104	14.500	25.132	71.476
RBF linear	1.490	7.157	14.631	22.783	50.584
RBF cubic	0.553	2.193	5.136	7.700	37.832
RBF thin plate spline	0.621	2.955	6.874	11.611	44.295
RBF quintic	0.555	2.045	4.064	5.649	**28.846**

- Local harmonic wins on all percentiles p50–p95 by a good margin
- At p99, RBF quintic is marginally better (28.8 vs 30.1 mT)
- Physics constraints allow it to perform better on points that are more difficult to reconstruct

Future Plans

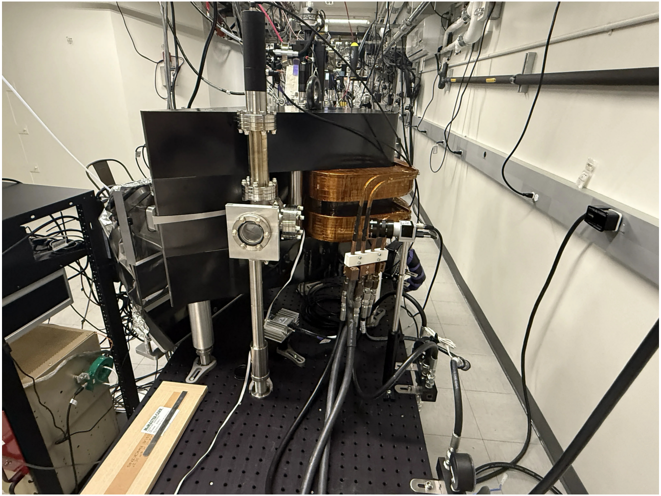

- Measure full PWFA energy spectrum
- Upgrade pole tips and core
- 2D gantry for magnetic field measurements